AGU PUBLICATIONS

JGR

Journal of Geophysical Research: Oceans

RESEARCH ARTICLE

10.1002/2016JC012326

Community production modulates coral reef pH and the sensitivity of ecosystem calcification to ocean acidification

Thomas M. DeCarlo[1,2], Anne L. Cohen[3], George T. F. Wong[4,5], Fuh-Kwo Shiah[5], Steven J. Lentz[3], Kristen A. Davis[6], Kathryn E. F. Shamberger[7], and Pat Lohmann[3]

[1]Massachusetts Institute of Technology and Woods Hole Oceanographic Institution Joint Program in Oceanography/Applied Ocean Science and Engineering, Woods Hole, Massachusetts, USA, [2]Now at School of Earth and Environment, The University of Western Australia, Crawley, Australia, [3]Woods Hole Oceanographic Institution, Woods Hole, Massachusetts, USA, [4]Department of Ocean, Earth and Atmospheric Sciences, Old Dominion University, Norfolk, Virginia, USA, [5]Research Center for Environmental Changes, Academia Sinica, Taipei, Taiwan, [6]University of California Irvine, Irvine, California, USA, [7]Texas A&M University, College Station, Texas, USA

Key Points:
- Benthic community photosynthesis dramatically increases daytime reef-water pH independent of the open ocean
- Diurnal-average net ecosystem calcification rates on Dongsha Atoll were exceptionally high compared to other coral reefs
- A transient coral bleaching event reduced net ecosystem metabolism and reef-water pH

Supporting Information:
- Supporting Information S1
- Data Set S1

Correspondence to:
T. DeCarlo,
thomas.decarlo@uwa.edu.au and
A. Cohen,
acohen@whoi.edu

Citation:
DeCarlo, T. M., A. L. Cohen, G. T. F. Wong, F.-K. Shiah, S. J. Lentz, K. A. Davis, K. E. F. Shamberger, and P. Lohmann (2017), Community production modulates coral reef pH and the sensitivity of ecosystem calcification to ocean acidification, *J. Geophys. Res. Oceans*, *122*, 745–761, doi:10.1002/2016JC012326.

Received 11 SEP 2016
Accepted 3 JAN 2017
Accepted article online 10 JAN 2017
Published online 31 JAN 2017

Abstract Coral reefs are built of calcium carbonate ($CaCO_3$) produced biogenically by a diversity of calcifying plants, animals, and microbes. As the ocean warms and acidifies, there is mounting concern that declining calcification rates could shift coral reef $CaCO_3$ budgets from net accretion to net dissolution. We quantified net ecosystem calcification (NEC) and production (NEP) on Dongsha Atoll, northern South China Sea, over a 2 week period that included a transient bleaching event. Peak daytime pH on the wide, shallow reef flat during the nonbleaching period was ~8.5, significantly elevated above that of the surrounding open ocean (~8.0–8.1) as a consequence of daytime NEP (up to 112 mmol C m^{-2} h^{-1}). Diurnal-averaged NEC was 390 ± 90 mmol $CaCO_3$ m^{-2} d^{-1}, higher than any other coral reef studied to date despite comparable calcifier cover (25%) and relatively high fleshy algal cover (19%). Coral bleaching linked to elevated temperatures significantly reduced daytime NEP by 29 mmol C m^{-2} h^{-1}. pH on the reef flat declined by 0.2 units, causing a 40% reduction in NEC in the absence of pH changes in the surrounding open ocean. Our findings highlight the interactive relationship between carbonate chemistry of coral reef ecosystems and ecosystem production and calcification rates, which are in turn impacted by ocean warming. As open-ocean waters bathing coral reefs warm and acidify over the 21st century, the health and composition of reef benthic communities will play a major role in determining on-reef conditions that will in turn dictate the ecosystem response to climate change.

1. Introduction

Coral reef ecosystems feed millions of people worldwide, provide shoreline protection, and generate trillions of dollars annually in tourism revenue [*Costanza et al.*, 2014]. Yet coral reefs are threatened by the rapid acidification of the oceans. Since the start of the industrial era, atmospheric CO_2 concentrations have increased at rates unprecedented for hundreds of millions of years [*Hönisch et al.*, 2012; *Zeebe et al.*, 2016], and more than one quarter of anthropogenic CO_2 emissions have already been absorbed into the oceans [*Sabine*, 2014], driving down ocean pH and aragonite saturation state ($\Omega_{Arag} = [CO_3^{2-}][Ca^{2+}]/K_{sp}'$ where K_{sp}' is the apparent solubility product in seawater), a process known as ocean acidification [*Doney et al.*, 2009]. Multiple studies have investigated coral reef calcification (net ecosystem calcification, or NEC) with techniques ranging from flow respirometry to inventories of species present and their individual calcification rates [*Odum and Odum*, 1955; *Kinsey*, 1985]. These studies consistently report correlations between NEC and reef-water Ω_{Arag}, and these relationships are used to forecast when ocean acidification will shift reefs from net accretion to net dissolution [*Ohde and van Woesik*, 1999; *Shamberger et al.*, 2011; *Shaw et al.*, 2012; *Bernstein et al.*, 2016; *Muehllehner et al.*, 2016]. Multidecade declines of NEC have already been observed on the Great Barrier Reef and attributed primarily to ocean acidification [*Silverman et al.*, 2012, 2014]. Supporting this assertion, *Albright et al.* [2016] artificially manipulated reef-water pH to levels of the preindustrial open ocean and found that NEC increased. If these results are representative of coral reefs worldwide, they imply that ocean acidification has already decreased NEC rates, and they raise concerns that this trend will endure into the next century as open-ocean pH continues to decline.

Such concerns are rooted in the assumption that reef-water pH tracks open-ocean pH. While the chemistry of open-ocean waters surrounding coral reefs appears to exert at least some influence on reef-water

chemistry [*DeCarlo et al*., 2015b; *Yeakel et al*., 2015], local benthic community metabolism (calcification and production) often drives significant changes [*Shaw et al*., 2012; *Cyronak et al*., 2014; *Shamberger et al*., 2014]. NEC represents the balance between calcification and dissolution, whereas net ecosystem production (NEP) represents the balance between photosynthesis and respiration

$$\text{NEC}: \quad Ca^{2+} + CO_3^{2-} \rightleftarrows CaCO_3, \tag{1}$$

$$\text{NEP}: \quad CO_2 + H_2O \rightleftarrows CH_2O + O_2 \tag{2}$$

As a result of community metabolism, the pH of water bathing corals may be higher [*Ohde and van Woesik*, 1999] or lower [*Shamberger et al*., 2014] than, and may not respond proportionally to [*Cyronak et al*., 2014], the pH of the open ocean. Accurate predictions of coral reef futures therefore require an understanding of the processes that control rates of community metabolism, reef-water carbonate chemistry, and any feedbacks between the two.

Chemical feedbacks between NEP and NEC are expected based on their relation with the seawater carbonate system. Community metabolism perturbs the carbonate system equilibria

$$H_2O + CO_2 \rightleftarrows H_2CO_3 \rightleftarrows H^+ + HCO_3^- \rightleftarrows 2H^+ + CO_3^{2-}, \tag{3}$$

where CO_2 (CO_3^{2-}) is produced from calcification (photosynthesis) because the removal of CO_3^{2-} (CO_2) shifts the carbonate system (equation (3)) to the left (right). Therefore, NEC and NEP are potentially linked because products of one are reactants of the other. This feedback system may have important ramifications for the sensitivity of coral reefs to ocean acidification. Photosynthesis by seagrass and algae has been proposed as a potential mechanism buffering coral reefs from ocean acidification because it removes CO_2 from reef water [*Kleypas et al*., 2011; *Smith et al*., 2013; *Andersson et al*., 2014]. However, the role of this chemical feedback system in modulating reef-water carbonate chemistry has so far been difficult to isolate because NEC, NEP, and reef-water pH are usually dominated by diurnal cycles that create strong correlations, but do not necessarily reflect causation [*Andersson and Mackenzie*, 2011]. Identifying the mechanistic, interactive links between community metabolism and reef-water carbonate chemistry is key for understanding the sensitivity of coral reef ecosystems to CO_2-driven climate change, including any compounding effects of ocean warming or changes in benthic community structure or health.

In this study, we investigated the drivers of reef-water carbonate chemistry and the metabolic rates of NEC and NEP on Dongsha Atoll, a remote coral reef in the northern South China Sea (SCS) (Figure 1). Here relatively high abundances of benthic flora and fauna on a wide and shallow reef flat impose dramatic changes in reef-water carbonate chemistry. We evaluate potential drivers of NEC, including elevated reef-water pH, coral community structure, and local oceanographic effects. Further, we tracked the community metabolism response to a transient, week-long coral bleaching event, which provided a novel opportunity to identify the sensitivity of reef-water carbonate chemistry, NEC and NEP to changes in community health and function. Overall, we explore potential links between NEC and NEP arising from chemical feedbacks within the seawater carbonate system, and we consider how changes in benthic community metabolism will modulate the sensitivity of coral reef ecosystems to future open-ocean acidification.

2. Methods

2.1. Study Location and Experimental Design

The SCS is a tropical to subtropical ocean basin extending from the equator to the Tropic of Cancer in the far western Pacific Ocean (Figure 1). A monsoon climate dominates the wind field in this region, with southwesterlies during the wet season from May to October, and northeasterlies during the dry season from November to April [*Wong et al*., 2007]. Surface ocean currents follow the wind pattern, with a basin-scale anticyclonic gyre in summer and a cyclonic gyre in winter [*Shaw and Chao*, 1994]. Within the centers of these gyres, high sea surface temperatures (>22°C throughout the year) produce a sharply defined pycnocline [*Shaw and Chao*, 1994; *Gawarkiewicz et al*., 2004], maintaining strong stratification and oligotrophic surface waters [*Wong et al*., 2007]. Coral reef ecosystems are abundant in the coastal waters of the South China Sea, including a portion of the Coral Triangle, the epicenter of coral reef biodiversity. Our study was conducted on Dongsha Atoll (20.8°N, 116.7°E), a ring-shaped coral reef ecosystem on the northern SCS

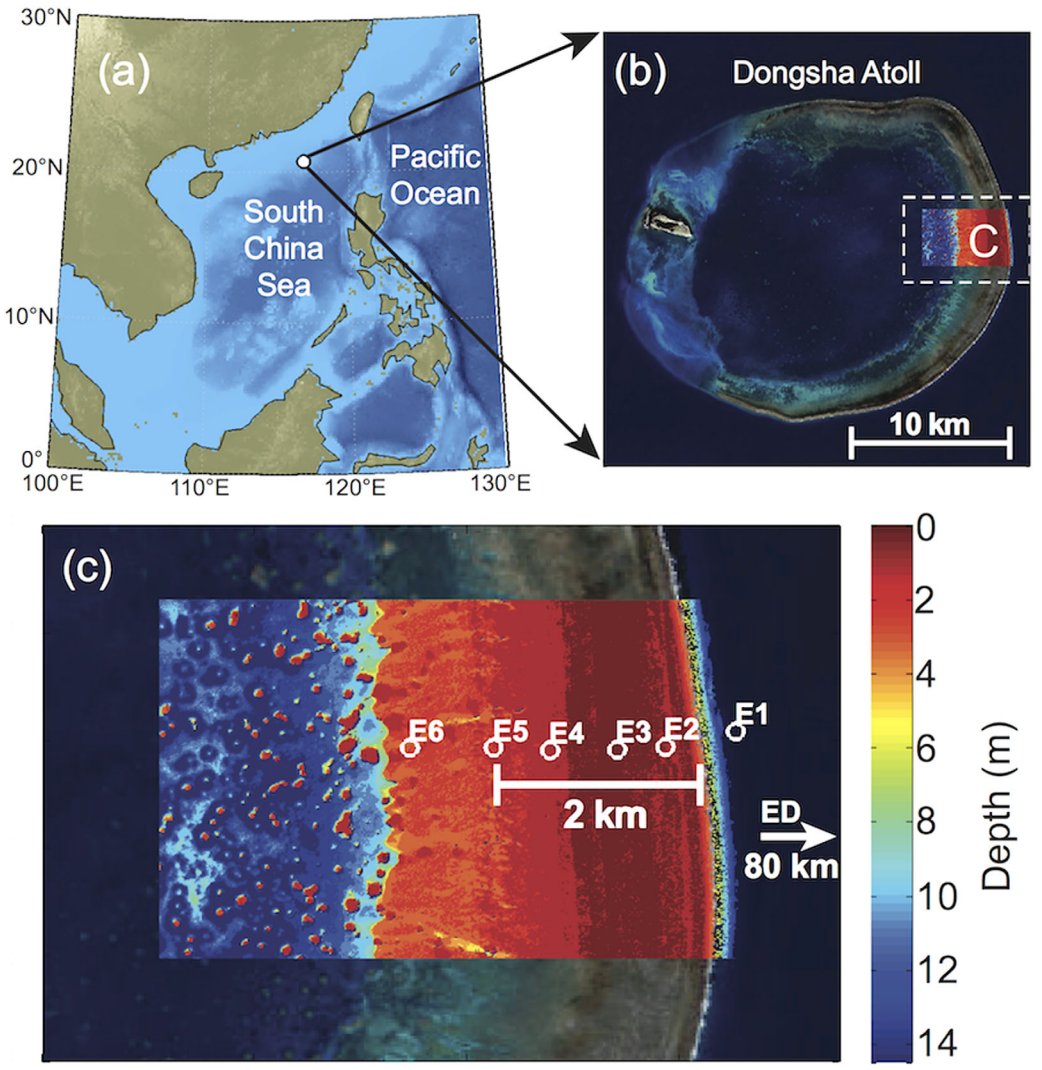

Figure 1. Map of Dongsha Atoll in the northern South China Sea. (a) Regional map, (b) satellite image of Dongsha Atoll from the Taiwan National Space Organization, and (c) study location and sampling stations on the eastern margin of the atoll. In Figure 1c, bathymetry data from *Shih et al.* [2011] are overlaid on the satellite imagery. Offshore samples were collected at station ED, located 80 km east of the atoll, and fore reef samples were collected at station E1. Instruments were deployed across the reef flat (Table 1), but the primary location for reef-water sampling was E5, located 2 km west of the reef crest.

shelf. On the western margin of the atoll is Dongsha Island, which is bordered to the north and south by 5 m deep channels into the large lagoon. Fringing the rest of the atoll is an extensive reef flat that is 1–3 m deep (Figure 1). Dongsha Atoll is unique in that it lies within the world's strongest internal wavefield [*St Laurent et al.*, 2011; *Fu et al.*, 2012; *Alford et al.*, 2015]. Large amplitude internal waves form on tidal frequencies in the Luzon Strait and propagate along the thermocline (70–100 m depth) as soliton depression waves westward into the northern South China Sea. As the internal waves interact with the shallow topography of the Dongsha Plateau, they transition into a train of elevation waves that bring subthermocline, nutrient-rich water to the otherwise oligotrophic sea surface [*Wang et al.*, 2007; *St Laurent et al.*, 2011], even reaching the coral communities of the Dongsha Atoll fore reef at depths of 10 m or less [*DeCarlo et al.*, 2015a].

We quantified ecosystem production and calcification rates based on tracking changes in carbonate chemistry as seawater flows from the open ocean, across the shallow reef flat of Dongsha Atoll. In June 2014, we collected seawater samples both offshore and on the eastern reef flat, while simultaneously characterizing the flow of water with current profilers. Additional data were collected to describe the benthic cover, and the physical setting on the reef flat, including photosynthetically active radiation (PAR), temperature, wind speed, and sea level. The instruments deployed and their roles in the experimental design are listed in Table 1, and the

Table 1. Experimental Design and Instrument Deployments

Site	Location	Depth (m)	Instruments/Activity	Purpose
ED	20.699°N 117.721°E	1200	Ocean Researcher 3 (OR3) water sampling station	Characterize background oceanic nTA and nDIC
E1	20.7008°N 116.9252°E	25	Seafet pH, SBE-37 T/S/O_2, SBE-56 thermistors on buoy at 10 m depth/OR3 water sampling station	Characterize carbonate chemistry of source-water to the reef
E2	20.6993°N 116.9186°E	0.8	SAMI pH, SBE-37 T/S, Seagauge P/Benthic survey	T/S properties of incoming water to the reef flat for nTA and nDIC calculations, local sea level from pressure/describe benthic community
E2.5	20.6992°N 116.9163°E	0.8	Benthic survey	Describe benthic community
E3	20.6991°N 116.9140°E	0.7	Nortek Aquadopp ADP/Benthic survey	Validate assumptions of conservative flow direction and transport across reef flat transect/describe benthic community
E3.5	20.6990°N 116.9109°E	0.7	Benthic survey	Describe benthic community
E4	20.6990°N 116.9077°E	0.8	Seagauge P/Benthic survey	Local sea level from pressure/describe benthic community
E4.5	20.6991°N 116.9051°E	0.9	Benthic survey	Describe benthic community
E5	20.6993°N 116.9024°E	2.0	Remote Access Sampler (RAS), SAMI pH, SBE-37 T/S, Nortek Aquadopp ADP, Onset Hobo U26 O_2, Wetlabs ECO-PAR, eKo meteorological station/Benthic survey	Collect water samples via RAS for NEC/NEP calculations, pH to validate TA/DIC collected in RAS, T/S properties of RAS samples to calculate ρ, O_2 to validate NEP, ADP to estimate reef water residence time, meteorological station to estimate CO_2 gas exchange rates/describe benthic community
E6	20.6993°N 116.8945°E	2.6	Seagauge P/Benthic survey	Local sea level from pressure/describe benthic community

benthic cover of calcifiers, seagrass, and algae are displayed in Table 2. We also observed a transient coral bleaching event on the reef flat in late May and early June 2014, in response to a 5°C temperature rise over the course of just 2–3 weeks (Figure S1). Although we did not precisely quantify the extent of bleaching, all of the massive *Porites* colonies, which compose ~30% of coral cover at station E5, appeared bleached. The bleaching event lasted less than 2 weeks, after which the coral colonies recovered their pigmentation.

Ecological surveys were conducted at eight stations across the eastern reef flat following a protocol similar to previously established methods for characterizing benthic cover on coral reefs [*Golbuu et al.*, 2007]. At each station, 5 × 50 m transect tapes were laid out and the seafloor was photographed every meter along each tape (0.5 m by 0.5 m image area), for a total of 250 photographs per station. Transects were oriented N-S (alongshore) and spaced 5 m apart (cross shore). Images were analyzed using Coral Point Count [*Kohler and Gill*, 2006] with five randomly placed points per image identified to coral genera or benthic substrate type (Table 2).

Bathymetry surveys were conducted across the reef flat between station E5 and the reef crest. A Reefnet Sensus Ultra pressure logger recording every 1 s was attached to a lead weight and dragged along the bottom following an E-W (cross shore) transect line. A Garmin 650 logging GPS was attached to a buoy and maintained above the pressure logger. We synced the depth and location data using the time logs from both the pressure logger and the GPS. The depth data were adjusted to mean sea level based on the local sea level at the time of surveying.

Table 2. Benthic Cover on the Eastern Reef Flat of Dongsha Atoll[a]

Site	CCA (%)	Fleshy Algae (%)	Sea Grass (%)	Live Coral (%)	*Acropora* (%)	*Pavona* (%)	*Porites* (%)	*Stylophora* (%)
E2	15	26	2	6	15	0	2	83
E2.5	4	17	10	24	24	0	29	47
E3	1	8	38	27	35	0	6	59
E3.5	1	10	37	23	40	0	1	59
E4	0	21	2	33	5	6	0	89
E4.5	0	34	13	16	41	9	17	33
E5	0	19	13	26	48	6	38	8
E6	0	3	78	0	0	0	0	0
Mean E2-E5	3	19	16	22	29	3	14	53

[a]The benthic types are reported as % areal cover, and coral genera are reported as % of total live coral cover.

2.2. Carbonate Chemistry Measurements

Seawater sampling was conducted on the fore reef (station E1) of Dongsha Atoll in order to characterize the total alkalinity (TA) and dissolved inorganic carbon (DIC) concentrations of seawater bathing the atoll. During 4–5 June 2014, seawater samples were collected at 2, 5, and 10 m depths every 3 h at station E1 using a Niskin bottle rosette deployed from the

Taiwanese vessel Ocean Researcher 3 (OR3). These samples were analyzed for TA, DIC, and salinity. Two additional surface water samples were collected at E1 from a small boat, one each on 3 and 18 June 2014. All TA/DIC samples were collected in 300 mL glass bottles and were immediately poisoned with 0.05–0.1 mL saturated $HgCl_2$ poison. Water samples were stored in the dark at ambient temperature and then returned to a shore-based laboratory for analysis. DIC was determined by measuring the infrared absorption of the CO_2 released upon the acidification of the sample by using an Apollo SciTech model AS-C3 DIC analyzer. TA was determined by an acidimetric Gran titration with an Apollo SciTech model AS-ALK2 alkalinity titrator. The precisions in the determination of TA and DIC were ± 2 μmol kg^{-1}. Details of the analyses are given in *Guo and Wong* [2015]. Salinity samples were collected in 125 mL glass bottles and analyzed with a Guildline autosal with a precision of ± 0.003.

On the reef flat, seawater samples were collected over multiple diurnal cycles at station E5 for carbonate chemistry analyses. A McLane Research Labs Remote Access Sampler-500 (RAS) was programmed to collect 450 mL seawater samples every 2 h in gastight Kynar Luer bags, in which 0.2 mL of saturated $HgCl_2$ poison was added prior to sampling (see *Shamberger et al.* [2011] for additional details regarding the application of the RAS for community metabolism measurements). Two 4 day RAS deployments were conducted, one during the transient bleaching event 3–6 June 2014 and another deployment postbleaching between 10 and 14 June 2014. Samples collected by the RAS were transferred to 300 mL glass bottles for transportation to the laboratory where TA and DIC were determined as in the discrete samples collected onboard the ship. Seawater density corresponding to each RAS sample was calculated with the standard 48-term equation [*McDougall et al.*, 2009], using temperature and salinity measured with a Seabird SBE-37 MicroCAT mounted on the RAS frame and calibrated against salinity measured in bottle samples. The TA and DIC of RAS samples, combined with temperature and salinity, were also used to calculate seawater pH, Ω_{Arag}, and pCO_2 using the program CO2SYS [*Lewis et al.*, 1998] with the acidity constants of *Mehrbach et al.* [1973] as refit by *Dickson and Millero* [1987].

The TA and DIC of our RAS samples were validated by comparison to hand-collected samples and to independent pH measurements. We collected seven discrete samples by opening bottles next to the RAS intake while the RAS collected samples. The average absolute differences in TA and DIC between the hand-collected samples and RAS samples were 11 and 10 μmol kg^{-1}, respectively, but with no significant biases (i.e., the mean TA and DIC from RAS samples were not significantly different from the bottle samples). In addition, we measured in situ pH (total scale) with a SAMI pH meter deployed alongside the RAS, and we used these data to calculate TA from measured DIC and pH, and to calculate DIC from measured TA and pH. Strong correlations were found between calculated and measured values (for TA, $r^2 = 0.97$ and reduced major axis (RMA) slope = 0.93; for DIC, $r^2 = 0.99$ and RMA slope = 0.95). We used the average absolute differences between measured TA and calculated TA (15 μmol kg^{-1}), and between measured DIC and calculated DIC (12 μmol kg^{-1}), as conservative estimates for uncertainties of TA and DIC in our RAS samples. While these uncertainties are several times larger than the analytical precisions, the TA and DIC changes in our study were large enough to clearly detect metabolic signals (mean absolute differences in TA and DIC between E1 and E5 were 84 and 133 μmol kg^{-1}, respectively).

Using our seawater samples, we quantified the relative influences of NEC and NEP on the seawater carbonate system (Figure 2). However, this information alone is insufficient to calculate metabolic rates for comparison to other reef systems. Only by coupling our TA and DIC measurements with estimates of reef water residence times can we quantify these rates.

2.3. Reef Water Residence Time

We estimated residence time of water flowing over the reef flat under a quasi-Lagrangian framework in which we traced the trajectories of water parcels across the reef indirectly with current velocity and bathymetry data. Current velocities were measured every 4 min at station E5 with a Nortek Aquadopp acoustic Doppler current profiler (ADP) (Figure 3). To test whether flow direction and transport ($q = \mathbf{u}h$) were conserved across the reef flat, a second ADP was deployed at station E3, approximately halfway between station E5 and the reef crest. We found that the major axis of flow direction was consistent within 2° and that transport was strongly correlated ($r^2 = 0.84$), but was 12% less at E3 compared to E5 (major axis regression slope = 0.88). This difference in transport across the reef flat can be explained by assuming that water flows inward toward the lagoon symmetrically around the ring of the atoll. Transport increases toward the lagoon-ward side of the reef flat because the perimeter of the inside of the reef flat is less than that of the outside edge of the atoll. We

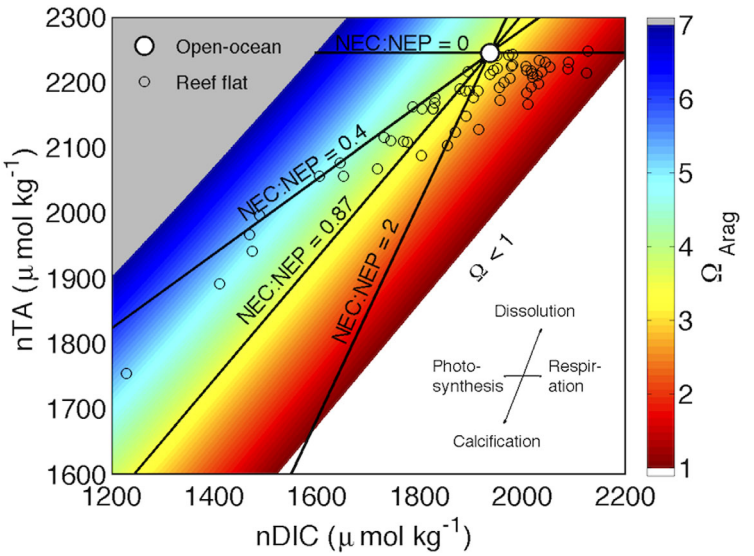

Figure 2. The seawater CO_2 system as a function of nDIC and nTA. Colors show Ω_{Arag} contours (calculated at 25°C), with white indicating undersaturation ($\Omega_{Arag} < 1$). The vector diagram in the lower right shows the predicted effects of community metabolic processes on TA and DIC. The large white circle shows the seawater composition of the open ocean surrounding Dongsha Atoll, the small open circles show our reef flat (station E5) measurements, and solid black lines show examples of the effects of NEC and NEP imposed on the offshore source-water for various NEC:NEP ratios. A NEC:NEP ratio of 0.87 maintains approximately constant Ω_{Arag}, whereas higher ratios decrease Ω_{Arag} and lower ratios increase Ω_{Arag}.

calculated the transport at any location on the reef flat based on the transport measured at E5 with the following expression:

$$q(x) = q_{E5}\frac{12,000 - x_{E5}}{12,000 - x}, \quad (4)$$

where q is transport, x is distance in meters from the reef crest toward the lagoon, q_{E5} is transport measured at station E5, and 12,000 m is the approximate distance from the reef crest to the center of the lagoon. Following this adjustment to transport across the reef flat, the mean difference in transport between E5 and E3 was <1%. This close agreement allows us to quantify the velocity at any location on the reef flat based on water depth and velocity at a fixed point (station E5). For each seawater sample collected at station E5, residence time (τ) of the sampled water parcel was estimated by back-tracking in time from E5 to the reef crest using depth-averaged cross-shore current velocity (**u**) and water depth (h) across the reef flat (Figure 3). The location x along the reef flat (i.e., distance from the reef crest) of a water parcel was estimated at any time t by

$$x(t) = \int_0^t \frac{\mathbf{u}_{E5}(t) \cdot h_{E5}(t)}{h(t,x)} dt, \quad (5)$$

where x is distance in meters from the reef crest, t is time in seconds, $\mathbf{u}_{E5}$ is the depth-averaged current velocity (m s^{-1}) measured by the ADP at station E5, h_{E5} is water depth at E5 based on pressure measurements from the ADP, and $h(t,x)$ is the local water depth at time t and location x along the path of each water parcel traversing the reef flat. In practice, equation (5) must be integrated stepwise from $x = 2020$ m (i.e., the distance from E5 to the reef crest) backward in time every 4 min (ADP sampling interval) until each water parcel is traced to the reef crest (Figure 3). With this approach, we calculated the residence time of each water parcel as the difference between the time that it crossed the reef crest and the time it was sampled by the RAS at station E5. The time-averaged depth of a water parcel is

$$\bar{h} = \frac{1}{\tau}\int_0^\tau h(t,x)dt, \quad (6)$$

which is calculated following the same stepwise approach described above.

Uncertainty of τ for each seawater sample was estimated with a Monte Carlo method, repeating the τ calculations 10^3 times while randomly adding measurement uncertainty in the current velocity ($1\sigma = 0.04$ m s^{-1} and assuming a Gaussian distribution) at each time step, and excluding any water parcels traced into the lagoon ($x = 3000$) or that traversed the reef crest at lowest spring tides when water depth at the reef crest was <30 cm and boulders on parts of the reef became emergent. This analysis yielded a total of 60 reliable measurements of paired NEC and NEP rates.

2.4. Reef Flat Metabolism

Community metabolic rates were quantified by combining estimates of reef-water residence time with measured carbonate chemistry changes. Exploiting the predictable ways in which community metabolism

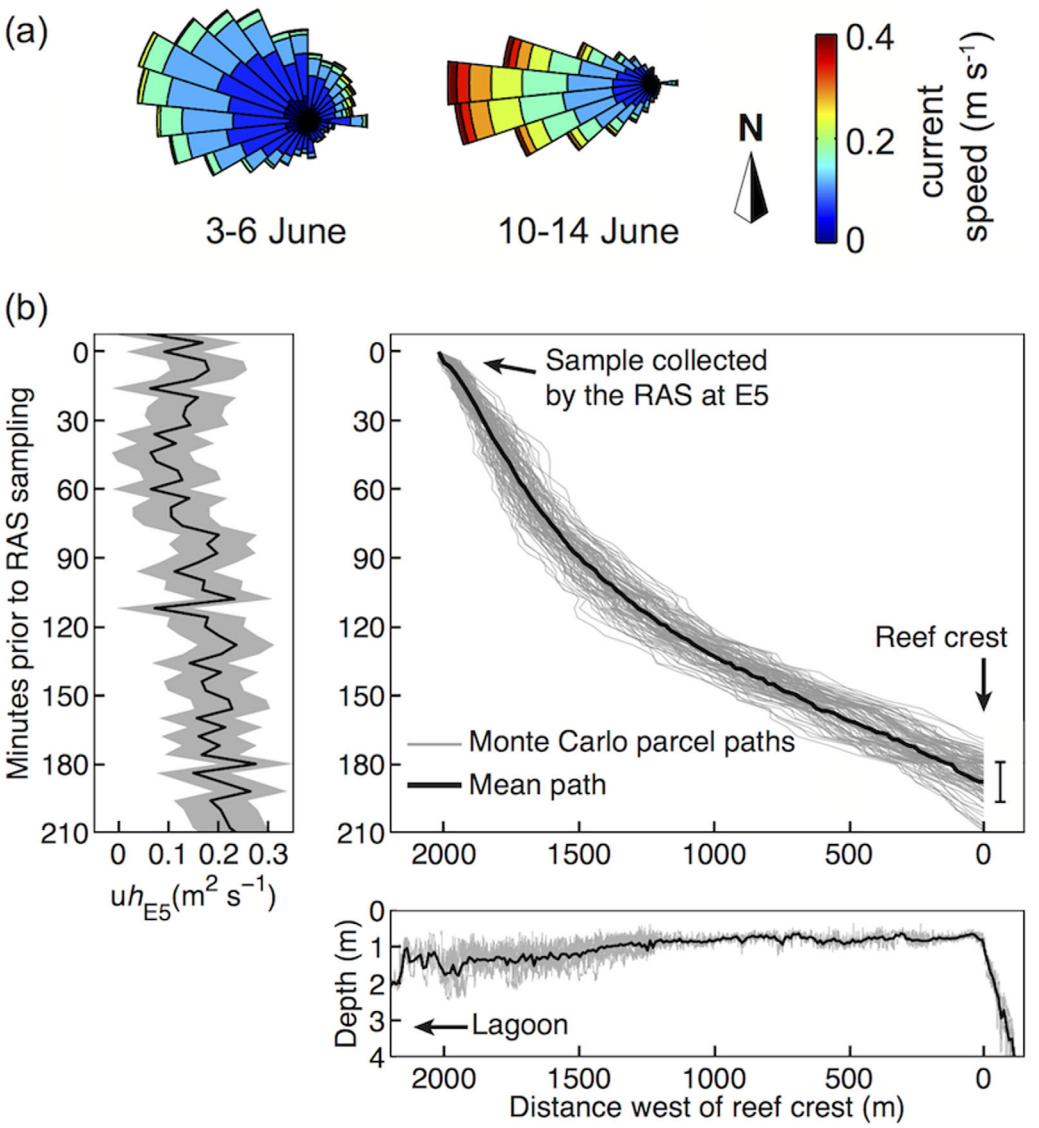

Figure 3. Reef water residence time. (a) Current velocities at station E5 during the two RAS deployments: 3–6 June and 10–14 June. The angle of each wedge indicates the compass direction of water flow, the length of each wedge indicates the relative frequency of currents flowing in that direction, and the colors on the wedge indicate the distribution of velocities in that direction. During 10–14 June, reef water was persistently flowing from the ocean toward to the lagoon (i.e., westward) but during 3–6 June, current direction switched between eastward and westward depending on the tide. (b) Quasi-Lagrangian calculation of reef water residence time. Left: transport (uh) measured at station E5 over 3.5 h during 10 June (positive westward). Gray error bounds represent measurement uncertainty of the ADP. Bottom: bathymetry profile across the reef flat. Gray lines represent individual bathymetry transects with ~1–3 m resolution. Thick black line shows mean bathymetry profile in 10 m horizontal bins. The RAS was located 2020 m from the reef crest. Main figure: seawater parcel tracing for one sample collected by the RAS on 10 June. Gray lines show the parcel trajectories for each of 100 Monte Carlo simulations. Tracing the seawater parcel begins with collection at the RAS, at known time and distance from the reef crest. The water parcel is then traced backward in time until it reaches the reef crest. Uncertainty in the current velocity at each time step imposes variability in parcel trajectories among Monte Carlo simulations. The thick black line shows the mean trajectory averaged across all iterations. The black error bar shows the 1σ uncertainty of residence time for this water parcel.

alters reef water carbonate chemistry (equations (1) and (2)), we can determine NEC and NEP rates by tracking changes in seawater TA and DIC over time [*Langdon et al.*, 2010]. Both TA and DIC are depleted by calcification, but only DIC is depleted by productivity. These metabolic rates are calculated as follows:

$$\mathrm{NEC} = \frac{\mathrm{nTA}_{E1} - \mathrm{nTA}_{E5}}{2\tau} \bar{h}\rho, \tag{7}$$

$$NEP = \frac{nDIC_{E1} - nDIC_{E5}}{\tau} \bar{h} \rho - NEC - F_{CO_2}, \quad (8)$$

where NEC and NEP are in units of mmol $CaCO_3$ m^{-2} h^{-1} and mmol organic carbon m^{-2} h^{-1}, respectively, nTA and nDIC are salinity-normalized TA and DIC, $\bar{h}$ is the time-averaged depth of the water parcel, ρ is seawater density (kg m^{-3}), τ is the residence time of a parcel of water on the reef (h), the factor 2 appears in the denominator of the NEC equation because two equivalents of TA are removed for each mole of $CaCO_3$ formed, and NEC is subtracted from NEP to account for the depletion (addition) of DIC by the precipitation (dissolution) of $CaCO_3$. While nTA_{E5} and $nDIC_{E5}$ were directly measured from RAS samples, nTA_{E1} and $nDIC_{E1}$ were calculated from the observed salinity/TA and salinity/DIC relationships on the fore reef. F_{CO2} is the CO_2 air-sea gas exchange flux (mmol CO_2 m^{-2} h^{-1})

$$F_{CO_2} = ks\rho(CO_{2\text{-water}} - CO_{2\text{-air}}), \quad (9)$$

where k is the gas transfer velocity (m h^{-1}), s is the solubility of CO_2 in seawater (mmol kg^{-1} atm^{-1}) calculated from temperature and salinity [*Weiss*, 1974], and $CO_{2\text{-air}}$ was assumed to be 400 μatm. The CO_2 transfer velocity is calculated with the parameterization of *Ho et al.* [2006] based on wind speed measured at 6 m mean altitude on a scaffolding tower constructed at station E5 and adjusted to 10 m altitude wind speed following the calculations of *Johnson* [1999], and converted to in situ temperature at salinity 35 following *Wanninkhof* [1992]. We estimated uncertainty in NEC and NEP rates by propagating uncertainty of offshore TA and DIC, reef flat TA and DIC, and τ. Mean relative standard deviations of NEC and NEP rates were 29 and 26%, respectively. The DIC-based NEP rates were validated by comparison to dissolved O_2-based NEP rates, following *Falter et al.* [2008] and using the constants of *Garcia and Gordon* [1992], *Johnson* [1999], *Sarmiento and Gruber* [2006], *Ho et al.* [2006], and *Turk et al.* [2015] (Supporting Information Figure S2).

3. Results

3.1. Open-Ocean Seawater Chemistry

The TA and DIC of each fore reef sample were normalized to salinity 34 (approximately the average offshore salinity) with the equations $nTA = \frac{34TA_{measured}}{S_{measured}}$ and $nDIC = \frac{34DIC_{measured}}{S_{measured}}$ for comparison to other studies of open-ocean carbonate chemistry. nTA and nDIC on the fore reef were 2241 ± 6 and 1936 ± 7 μmol kg^{-1} (1 σ), respectively. These results are within uncertainty of nTA and nDIC in samples collected at 10–20 m depth at station "ED" located in the open-ocean 80 km east of Dongsha Atoll (nTA of 2240 ± 2 μmol kg^{-1} and nDIC of 1927 ± 3 μmol kg^{-1}), and within uncertainty of other published relationships between TA/DIC and salinity for the tropical Pacific Ocean (*Lee et al.* [2006] relationship predicts nTA of 2239–2243 μmol kg^{-1} between 25 and 30°C) and the South China Sea (*Guo and Wong* [2015] relationship predicts nTA of 2249 ± 8 μmol kg^{-1} and nDIC of 1940 ± 9 μmol kg^{-1}). The consistency between our fore reef, open-ocean, and published nTA and nDIC values gives us confidence that our nTA and nDIC estimates on the Dongsha Atoll fore reef are representative of the background oceanic composition and that we can reliably estimate nTA and nDIC of water flowing onto the reef for times when only salinity, and not TA or DIC, was measured.

3.2. Reef Flat Metabolism

We calculated NEC and NEP based on our nTA and nDIC measurements at station E5, combined with estimates of water residence time on the reef flat. Reef-water residence times varied between 1 and 7 h, nTA varied between 1754 and 2247 μmol kg^{-1}, and nDIC varied between 1229 and 2127 μmol kg^{-1} at station E5 (Figure 2). NEC and NEP rates also changed throughout the course of a day (Figure 4). Maximum NEC and NEP rates typically occurred in late afternoon, approximately the same time as maximum O_2, pH, and Ω_{Arag} (Figures 5 and 6). During nighttime, NEC decreased to near zero, but we observed no significant net dissolution, which contrasts with most coral reefs studied to date (Table 3). Conversely, nighttime NEP was consistently negative (net respiration). NEP rates calculated based on O_2 stoichiometry were in close agreement with the carbon-based estimates (Figure S2). Minimum O_2, pH, and Ω_{Arag} all occurred shortly before dawn. Throughout our study, the ranges of NEC and NEP were between 0 and 44 mmol $CaCO_3$ m^{-2} h^{-1}, −73 and 112 mmol C m^{-2} h^{-1}, and the ranges of seawater chemical properties were O_2 0–18 mg L^{-1}, pCO_2 76–1520 μatm, pH 7.3–8.5, and Ω_{Arag} 1.3–5.6 (Figures 4–6).

The multiday metabolic rate time series were compiled to estimate diurnal-average NEC and NEP for comparison with other coral reef systems worldwide (Table 3). During 10–14 June, persistent westward currents

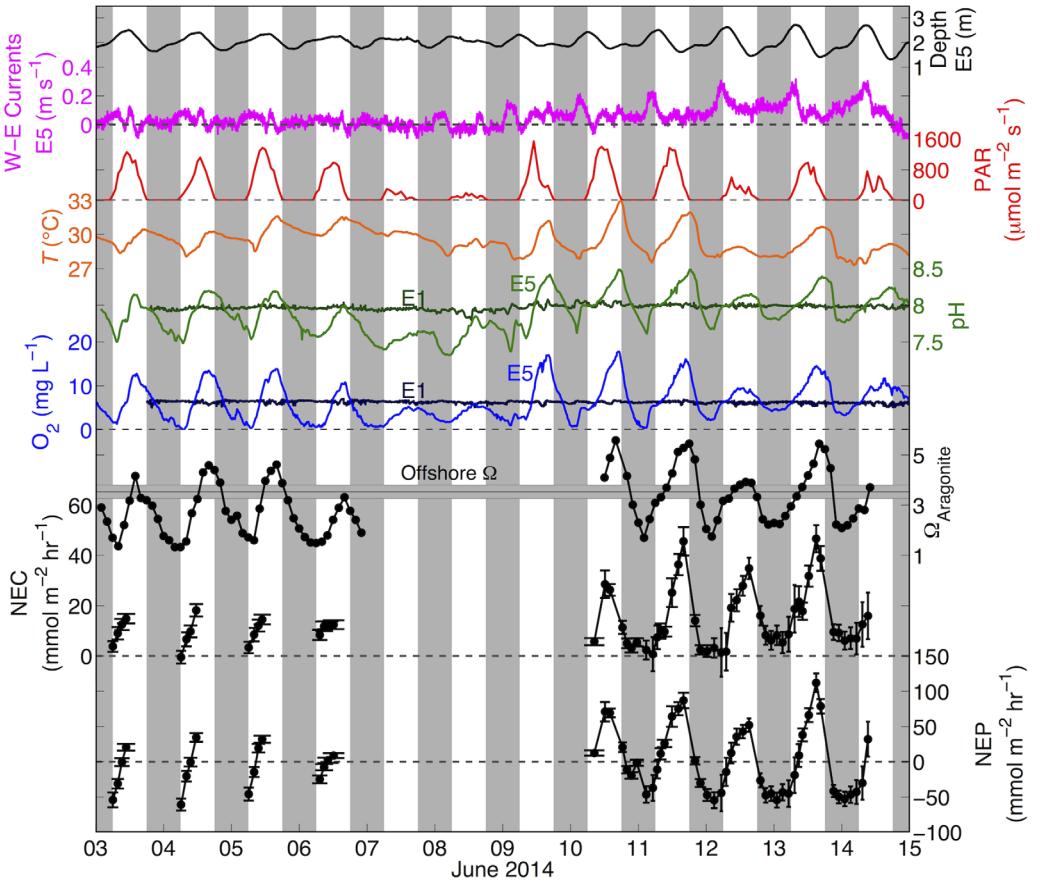

Figure 4. Time series of physical and chemical properties, and metabolic rates on the Dongsha Atoll reef flat in June 2014. From top to bottom: sea level, current speeds (positive westward, negative eastward), PAR, temperature, pH, O_2, Ω_{Arag}, NEC, and NEP. For pH and O_2, lighter colors show reef flat measurements at station E5 and darker colors fore reef measurements at station E1. Mean offshore Ω_{Arag} and its 1σ are plotted as the black horizontal line with gray error bound. NEC and NEP are plotted with vertical error bars representing the uncertainty of the rates and the width of these error bars representing the time over which each measurement represents (i.e., the residence time). Horizontal dashed lines show 0 rates that separate calcification from dissolution and photosynthesis from respiration.

allowed us to capture full diurnal cycles. However, during 3–6 June westward flow occurred only during flood tides, and as a result our metabolic rate measurements only span daylight hours (Figures 5 and S4). Therefore, we compare rates between 3–6 June and 10–14 June for the overlapping times of day, but we use only 10–14 June measurements to estimate diurnal-averaged metabolic rates. Mean metabolic rates were calculated in 2 h bins and integrated over 24 h (Figure 5). This resulted in diurnal-average NEC of 390 ± 90 (1 standard error) mmol $CaCO_3$ m^{-2} d^{-1} and NEP of 100 ± 300 mmol C m^{-2} d^{-1}.

We evaluated the effect of coral bleaching on the community metabolic rates by comparing NEC and NEP during the bleaching event (3–6 June) to postbleaching (10–14 June). Since our measurements during the bleaching event only span a portion of the diurnal cycle, we calculated the differences between the measured 3–6 June metabolic rates and the rates expected at the same times of day based on the 10–14 June diurnal cycle (Figure 5). The residual NEC (-7 ± 1 mmol $CaCO_3$ m^{-2} h^{-1}) and NEP rates (-29 ± 3 mmol C m^{-2} h^{-1}) were significantly ($p < 0.05$) different from zero, meaning that metabolic rates were reduced during the bleaching event relative to postbleaching. Further, we tested whether the reduced NEC and NEP rates during bleaching were attributable to any differences in abiotic factors. We found that for any PAR or temperature level, NEC and NEP rates were lower during bleaching than postbleaching, and multiregression analysis accounting for the combined influence of PAR, temperature, current speeds, sea level, and water depth still produced significant effects of bleaching on the metabolic rates (Supporting Information).

NEC and NEP were significantly ($p < 0.05$) positively correlated with both linear and exponential type II (major axis) regressions (Figure 7). However, investigation of the residuals of the linear regression showed

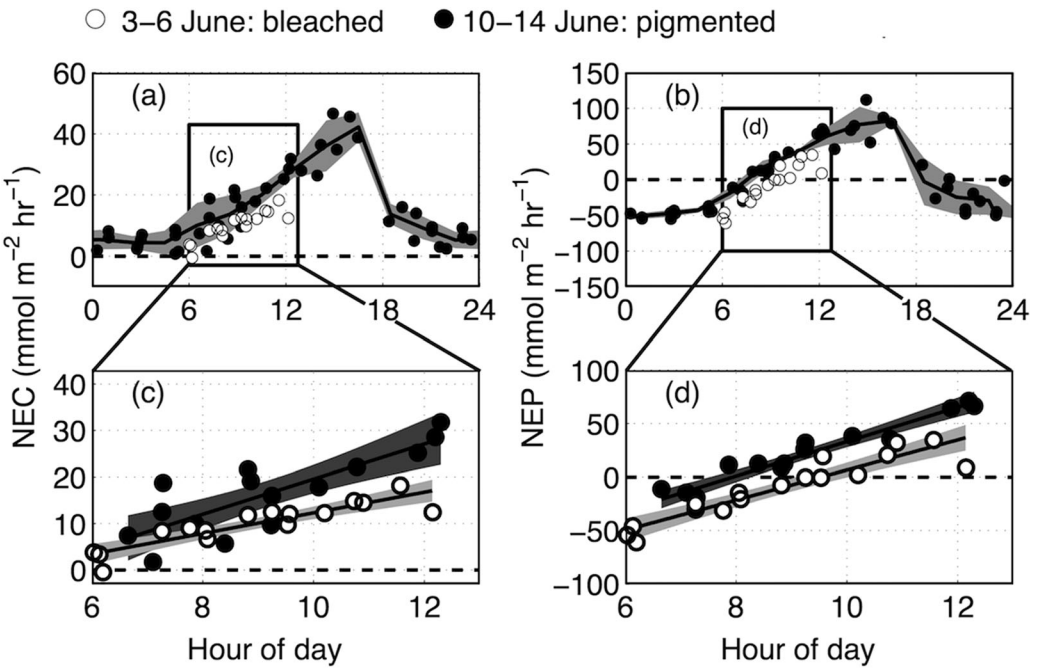

Figure 5. Diurnal compilations of (a, c) NEC and (b, d) NEP rates. Dashed horizontal lines indicate 0 rates that separate net calcification from dissolution and net photosynthesis from respiration. White and black circles indicate 3–6 June (during bleaching) and 10–14 June (postbleaching) measurements, respectively. In Figures 5a and 5b, the solid black line and gray shading represent the mean rates $\pm 1\sigma$ in 2 h bins, calculated using only the postbleaching data. (c, d) Measurements during bleaching and postbleaching overlap between approximately 06:00 and 12:30, and over this time the NEC and NEP rates during bleaching are significantly reduced (see section 3). Solid black lines are linear regression fits, and light and dark shading are 95% confidence intervals for during and postbleaching data, respectively. All points are plotted on the time axis as the midpoint between when the water parcel traversed the reef crest and the sampling time (see Supporting Information for further details).

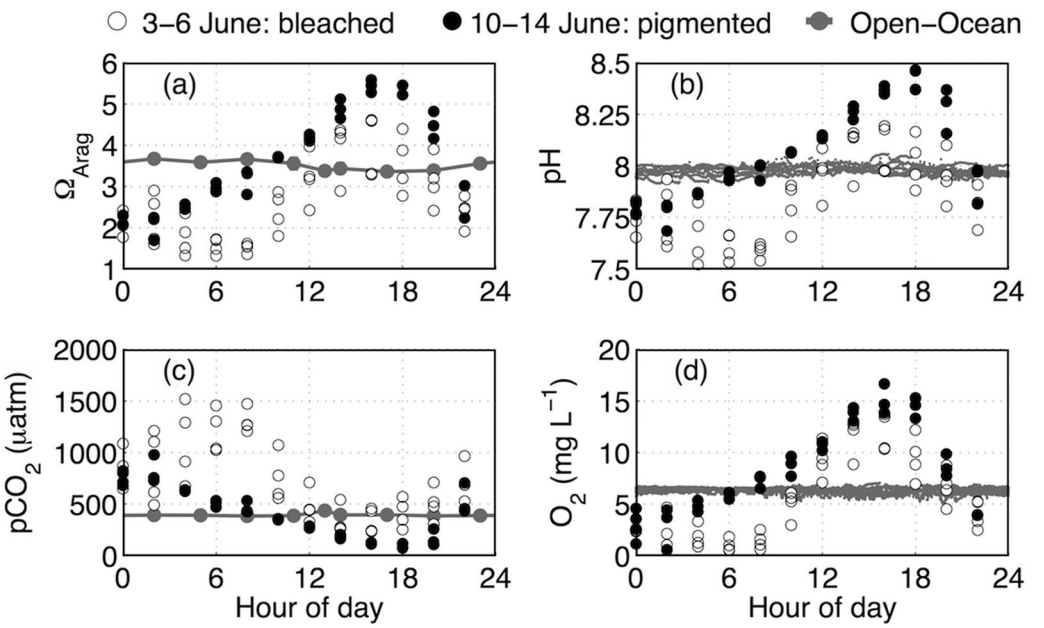

Figure 6. Diurnal compilations of seawater (a) Ω_{Arag}, (b) pH, (c) pCO_2, and (d) dissolved O_2. Open and filled black circles indicate 3–6 June (during bleaching) and 10–14 June (postbleaching) measurements, respectively, on the reef flat at station E5, and gray points are open-ocean measurements from station E1 over the same time period as the reef flat measurements. The reef flat data were derived from RAS samples and an O_2 sensor at E5, open-ocean pH and O_2 were measured at E1, and open-ocean Ω_{Arag} and pCO_2 were calculated from OR3 samples. Ω_{Arag} and pH are greatly elevated on the reef flat during the day, and in comparison they change relatively little in the surrounding open ocean. These carbonate system parameters follow similar diurnal patterns during and after the bleaching event, but they are all significantly ($p < 0.05$; two-sample t tests) different during bleaching (pH, Ω_{Arag}, and O_2 decreased; pCO_2 increased).

Table 3. Global Compilation of NEC and NEP Rates Measured on Coral Reefs

Study	Location	NEC (mmol m^{-2} d^{-1})	Max NEP (mmol m^{-2} h^{-1})	Coral/Calcifier Cover (%)	Open-Ocean Ω_{Arag}	Reef Type/Method
Kinsey [1985]		109				Literature review
Barnes and Lazar [1993]	Red Sea	163[a]	<80	~100	4[a]	Fringing reef, Lagrangian method
Gattuso et al. [1993]	Moorea	243	<100	2–31	*3.9*	Barrier reef, Lagrangian method
Gattuso et al. [1996]	Moorea	186[b]	<100	2–31	*3.9*	Barrier reef, Lagrangian method
	Great Barrier Reef (GBR)	253[b]	<150	30	*3.1*	Barrier reef, Lagrangian method
Kraines et al. [1997]	Japan	167–317[a]	50	0–20	*3.6*	Reef flat and lagoon, quasi-Lagrangian
Ohde and van Woesik [1999]	Japan (daytime)	127–312	18	37	4.47	Reef flat and lagoon, slack-tide method
Langdon et al. [2003]	Biosphere-2	41	<50	3	2.83	Mesocosm
Kayanne et al. [2005]	Japan	70–127[a]	<100	5.8–7.1	*3.5*	Barrier reef flat, quasi-Lagrangian
	Palau	74–130[a]	<100	1.4–8.1	*3.9*	Barrier reef flat, quasi-Lagrangian
Langdon and Atkinson [2005]	Hawaii	370–380	<80	100	3	Mesocosm
Yates and Halley [2006]	Hawaii	−7.2 to 3[a]		10–22	*3.5*	Mesocosm/enclosure
Silverman et al. [2007]	Red Sea	−4 to 108[a]		20–40	4	Fringing reef, Eulerian
Andersson et al. [2009]	Hawaii	79[a]		20–30	2.8	Mesocosm
Bates et al. [2010]	Bermuda	−22 to 104		21	3.7	Barrier reef and lagoon
Shamberger et al. [2011]	Hawaii	235–293[a]	<80	20–30	*3.9*	Barrier reef flat, quasi-Lagrangian
Falter et al. [2012]	W Australia	190–200[b]	<150	50–90	*3.6*	Reef flat, Eulerian
Shaw et al. [2012]	GBR	145[a]	<40	40	*3.5*	Reef flat and lagoon, slack-tide method
Silverman et al. [2012]	GBR	74–133[a]	<63	14–15	3.65	Reef flat and lagoon, slack-tide method
Albright et al. [2013]	GBR	77–166[a]	<75	17–18	*3.1*	Reef flat, Lagrangian
McMahon et al. [2013]	GBR	58[a]	113	<15	*3.5*	Lagoon, slack-tide method
Teneva et al. [2013]	Palau	33.8[a]			*3.9*	Backreef, control volume
Jokiel et al. [2014]	Hawaii	144[a]		~100		Mesocosm
Lantz et al. [2014]	Hawaii	80[a]	40	10–17	*3.5*	Reef flat, quasi-Lagrangian
Silverman et al. [2014]	GBR (1975–1976)	83–105[a]		8	3.6	Reef flat, quasi-Lagrangian
	GBR (2008–2009)	54–61[a]		8		Reef flat, quasi-Lagrangian
Albright et al. [2015]	GBR	104[a]	61	35	*3.5*	Reef flat, Lagrangian
Koweek et al. [2015b]	American Samoa	216		46	4.06	Lagoon pools, quasi-Lagrangian
Longhini et al. [2015]	Brazil	58–197[a]	<70	5–50	*3.8*	Reef flat, slack-tide method
Shaw et al. [2015]	GBR	33[a]	<30	25	3.41	Reef flat, slack-tide method
Turk et al. [2015]	Florida	−35 to 50[a]	13	25	3.7	Mesocosm/enclosure
Bernstein et al. [2016]	Red Sea	110	72	61	4.6	Reef flat, Eularian
Courtney et al. [2016]	Bermuda	61–64		28	3.7	Rim reef, census and chemical
Kwiatkowski et al. [2016]	GBR	36[a]	<40	18	3.65	Reef flat, slack-tide method
Muehllehner et al. [2016]	Florida	−7 to 17		2–7	3.7	Patch Reefs, Be-7 method
Takeshita et al. [2016]	Palmyra Atoll	18–118[a]	23	30–70	*3.9*	Back reef, benthic gradient flux method
This study	Dongsha Atoll	390 ± 90[b]	112	25	3.4	Reef flat, quasi-Lagrangian

[a]Indicates nighttime net dissolution occurred.

[b]Indicates nighttime net dissolution did not occur. Ocean Ω_{Arag} is from data presented in each study, if offshore (i.e., open-ocean) samples were collected. For studies without offshore sampling, Ω_{Arag} values were calculated from climatology and are displayed in italics. Climatological Ω_{Arag} was derived for the nearest 1° by 1° grid box with temperature, salinity, nitrate, phosphate, and silicate climatologies from World Ocean Atlas [*Levitus*, 2010] and the DIC climatology of *Key et al.* [2004]. TA was calculated from temperature and salinity with open-ocean relationships [*Lee et al.*, 2006], and Ω_{Arag} was calculated using the program CO2SYS [*Lewis et al.*, 1998] and the acidity constants of [*Mehrbach et al.*, 1973] refit by [*Dickson and Millero*, 1987]. *Koweek et al.* [2015a] also measured NEC on Palmyra Atoll with Lagrangian and Eulerian methods, but because the reported uncertainties are generally larger than the NEC signals, and the overlapping Lagrangian and Eulerian measurements differ by a factor of more than 2, it is difficult to estimate the diurnal-average NEC rate.

clear structure and the NEC residuals were significantly correlated with NEP using a second-order polynomial, whereas NEC residuals of the exponential regression showed no clear structure and produced no significant correlation with NEP. The best fit equation (±2 σ) was

$$\mathrm{NEC} = e^{0.016(0.003)\mathrm{NEP}+2.3(0.1)}, \quad (r^2 = 0.83,\ p < 0.01), \tag{10}$$

where NEC and NEP are in units of mmol $CaCO_3$ m^{-2} h^{-1} and mmol C m^{-2} h^{-1}, respectively. There was no significant difference in the NEC to NEP relationship during and postbleaching (Figures 7, S5, and S6).

4. Discussion

4.1. Interaction Between Carbonate Chemistry and Community Metabolism

Anthropogenic CO_2 emissions are forecast to drive changes in pH and Ω_{Arag} of 0.3 and 1.5 units, respectively, in surface waters of the tropical oceans by the end of the 21st century. These waters bath coral reefs, and the changes driven by ocean acidification are projected to cause declines in ecosystem calcification rates [*Shamberger et al.*, 2011; *Shaw et al.*, 2012; *Bernstein et al.*, 2016]. Yet these projections do not account for

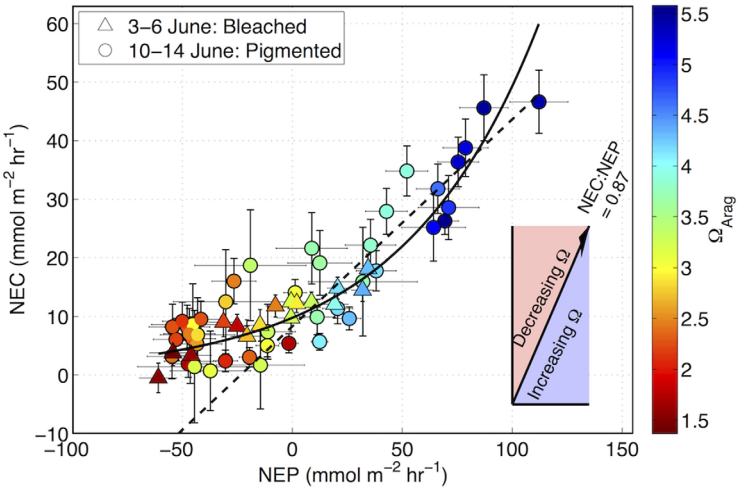

Figure 7. Interactive relationship between NEC, NEP, and Ω_{Arag}. Triangles and circles indicate 3–6 June (bleaching) and 10–14 June (postbleaching) measurements, respectively, and colors show Ω_{Arag} at station E5. Solid black line is exponential fit between NEC and NEP. Theoretical vector in lower right shows the slope between NEC and NEP (0.87) that maintains an approximately constant Ω_{Arag}. Greater slopes decrease Ω_{Arag} and lesser slopes increase Ω_{Arag}. The exponential curve is increasing in slope at higher NEP, but is always less than the 0.87 critical value, and thus the highest Ω_{Arag} values correspond to the highest NEC and NEP rates. The dashed black line shows a linear fit between NEC and NEP for only daylight hours (NEC:NEP is 0.35) and extrapolated to all hours of the day, showing that net dissolution would be expected during night based on the daytime relationship. Even though respiration drives down Ω_{Arag} to <2 during nighttime, net dissolution did not occur. The 10–14 June data cover full diurnal cycles, but the 3–6 June data cover only 06:00 to 12:30. Thus, while this figure shows that the relationship between NEC and NEP is maintained during bleaching, it cannot be used to interpret changes in diurnal-average NEC and NEP rates. See Supporting Information for comparisons of NEC and NEP between 3–6 June and 10–14 June only during the common hours of day.

the potentially compounding effects of ocean warming or the processes that differentiate reef-water and open-ocean chemistry. Predicting the sensitivity of coral reef ecosystems to CO_2-driven climate changes requires an understanding of the interactions between open-ocean acidification and the processes driving carbonate system changes in reef waters.

As open-ocean seawater flows onto coral reefs, benthic communities alter its carbonate chemistry. The reef flat of Dongsha Atoll is shallow (~1–3 m), wide (~3 km), and has high live benthic cover (61% combined coral, algae, and seagrass). TA and DIC fluxes are imposed by most of the benthic area (high living cover), chemical changes accumulate rapidly in the shallow water column, and these changes are integrated as seawater traverses the wide reef flat. On the Dongsha reef flat at station E5, TA and DIC depletions relative to the surrounding open ocean were as high as 481 and 707 μmol kg^{-1}, respectively (Figure 2), greater than those measured in water flowing across other coral reefs with similar residence times and bathymetry [*Shamberger et al.*, 2011; *Shaw et al.*, 2014; *Silverman et al.*, 2014].

Due to these changes in reef-water chemistry, calcifiers on the Dongsha reef flat build their shells and skeletons in seawater with elevated pH and Ω_{Arag}. The vast majority of NEC (80%) occurs during daytime, when reef-water pH and Ω_{Arag} reach as high as 8.5 and 5.5, respectively, compared to ~8.0 and ~3.4 in the surrounding open ocean (Figure 6). Under these conditions, the diurnal-average NEC rate on Dongsha Atoll was greater than that measured for other coral communities studied to date (Table 3 and Figure 8). On average worldwide, reef flat NEC rates are ~110–130 mmol $CaCO_3$ m^{-2} d^{-1} [*Kinsey*, 1985; *Atkinson*, 2011], and the highest diurnal-average NEC rate previously measured in the field was 290 mmol $CaCO_3$ m^{-2} d^{-1} [*Shamberger et al.*, 2011]. Conversely, we measured diurnal-average NEC of 390 mmol $CaCO_3$ m^{-2} d^{-1} on the Dongsha reef flat. Although our measurements do not capture seasonal changes, the June NEC rate on Dongsha Atoll is uniquely high relative to all seasons on other coral reefs, and this is not explained by calcifier cover or coral community structure. The calcifier cover on the Dongsha reef flat (25%) is similar to other reefs where NEC has been measured (Table 3 and Figure 8), and even though community structure data are not available for most metabolism studies, the relatively high abundance of fast-growing *Acropora* and *Stylophora* [*Dullo*, 2005] on Dongsha is similar to that of other reefs with lower NEC rates [e.g., *Gattuso et al.*, 1996]. It is possible that the high NEC rates were a result of exceptional metabolism during the recovery from the coral bleaching event, but more studies of community metabolism before, during, and after bleaching events are needed to evaluate this hypothesis. Another possibility is that large internal waves colliding with the atoll deliver nutrient-rich waters that stimulate rapid metabolism [*DeCarlo et al.*, 2015a]. Nevertheless, our findings of extremely high NEC on Dongsha Atoll contrast with the paradigm that healthy coral reefs with favorable conditions for calcification have low algal cover and high open-ocean Ω_{Arag}

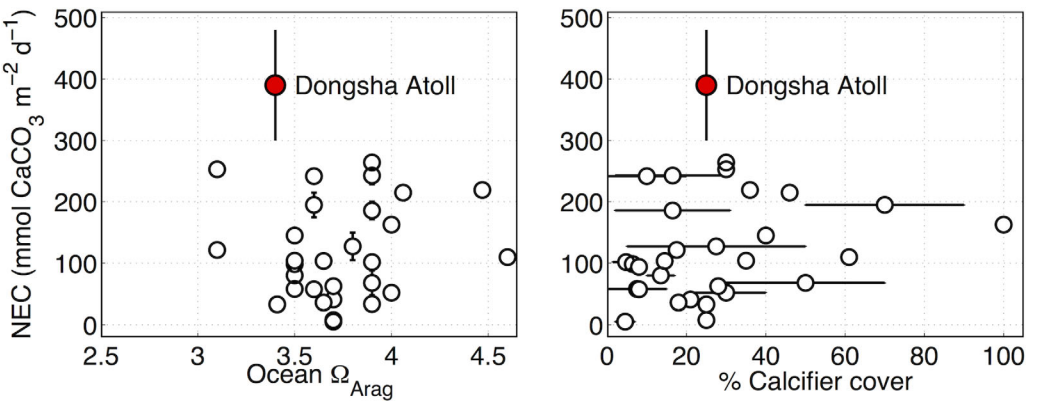

Figure 8. Global compilation of coral reef diurnal-average NEC rates plotted as functions of open-ocean Ω_{Arag} and % calcifier cover. Despite relatively low open-ocean Ω_{Arag} and comparable calcifier cover, NEC rates on Dongsha Atoll are significantly higher than those of all other reef systems studied to date. The data sources are tabulated in Table 3.

[*Hoegh-Guldberg et al*., 2007]. Rather, the benthic cover of fleshy algae on the Dongsha reef flat is relatively high (19%) compared to most Indo-Pacific reefs [*Bruno et al*., 2009; *Roff and Mumby*, 2012], and the open-ocean Ω_{Arag} (~3.4) in the northern South China Sea is near the minimum associated with most tropical coral reefs today [*Hoegh-Guldberg et al*., 2007].

Daytime photosynthesis plays a key role in sustaining chemical conditions favorable for rapid calcification on the Dongsha reef flat. The NEC rates are so high that they alone would drive daytime Ω_{Arag} toward saturation ($\Omega_{Arag} = 1$), and sometimes even below (Figure 9). We observed the opposite response, however, with daytime Ω_{Arag} rising to greater than 5 on the reef at the same time of day as the most rapid NEC (Figures 4–6). This is explained by the effect of NEP on the seawater carbonate system. Using our diurnal measurements of coupled TA and DIC changes, we isolated the effects of NEC and NEP on reef-water carbonate chemistry. Our analysis indicates that daytime $[CO_3^{2-}]$ is elevated eightfold under the combined effects of NEC and NEP compared to the isolated effect of NEC (Figure 9). NEP removes CO_2 from reef water, preventing aragonite under-saturation ($\Omega_{Arag} < 1$) that would favor dissolution over calcification. Correlations between NEC and NEP are a common feature both within [*Shaw et al*., 2012; *Albright et al*., 2015; *Koweek et al*., 2015b], and among [*Gattuso et al*., 1999], coral reef communities. Likewise, we observed this link on Dongsha Atoll, where it is maintained even at extremely high NEC and NEP rates (Figure 7). These results highlight the important function of primary producers in modulating carbonate chemistry of coral reef waters.

Community metabolism on Dongsha Atoll is also unique in that NEC increases exponentially, rather than linearly, with increasing NEP (Figure 7). Related to this exponential relationship, we found that NEC decreases to near zero at night but we found no significant net dissolution, which is rare among coral reef community

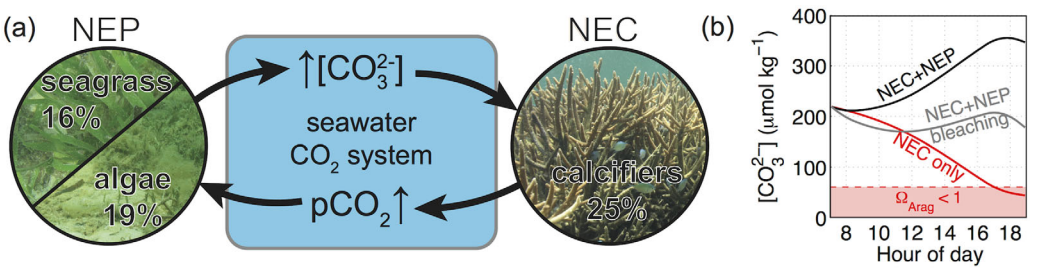

Figure 9. (a) Schematic diagram showing that NEP elevates $[CO_3^{2-}]$, which is consumed by NEC. In turn, NEC elevates CO_2, which is consumed by NEP. (b) Daytime profile of calculated reef-water $[CO_3^{2-}]$ with isolated and combined effects of NEC and NEP. The calculations were performed for a 1 m water column with residence time on the reef flat from dawn to dusk. Thus, the differences between curves show effects of community metabolism and are not dependent upon residence times. The black curve is the calculated effect of NEC and NEP, the red curve shows the $[CO_3^{2-}]$ profile with the isolated effect of NEC, and the gray curve shows the combined effects of NEC and NEP during the bleaching event (when NEC and NEP were reduced by 7 and 29 mmol m^{-2} h^{-1}, respectively). The isolated effect of NEC on $[CO_3^{2-}]$ is so strong that it alone would drive Ω_{Arag} to under-saturation (light red shading).

metabolism studies (Table 3). In fact, the lack of nighttime dissolution is partly responsible for the uniquely high NEC rates on Dongsha Atoll (Figure 7), as diurnal-average NEC on most other reefs is a balance between net calcification during the day and net dissolution at night. Because our data reveal only the net rates, we cannot determine if dissolution is entirely absent on the reef flat or if nighttime dissolution is balanced by nighttime calcification. Identifying the factors that influence dissolution is thus a key question in understanding net $CaCO_3$ production on Dongsha Atoll, and in coral reef ecosystems generally. Future studies of coral reef community metabolism may benefit by combining methods similar to ours for the net rates with techniques to quantify certain components of the metabolic signals, such as by using benthic flux chambers to measure dissolution in sediments [*Andersson and Gledhill*, 2013; *Cyronak et al*., 2013].

4.2. Effects of Bleaching on Community Metabolism

The role that the benthic community plays in modulating carbonate chemistry of reef water is further evident from changes in community metabolism associated with thermal stress. Anomalously high, or rapidly increasing, temperature can induce coral bleaching, the loss of the symbiotic algae from the coral holobiont [*Glynn*, 1993]. Coral mortality following bleaching has been shown to reduce NEC rates [*Kayanne et al*., 2005], but no data exist to evaluate changes in community metabolism during a bleaching event. On Dongsha Atoll, reef-water temperature increased by 5°C in less than 3 weeks during May 2014, and by the beginning of June most of the massive corals had bleached (Figure S1). As reef waters cooled, bleaching subsided and corals regained their symbiotic algae populations by mid-June.

During the transient bleaching event, NEP decreased by 29 mmol m^{-2} h^{-1} and NEC decreased by 7 mmol m^{-2} h^{-1}, a 40% reduction compared to the nonbleaching measurements (Figure 5). Yet bleaching is not the only possible explanation for these changes. Rates of community metabolism are naturally variable and the percent differences between bleaching and nonbleaching periods that we observed are within the range of natural variability recorded on weekly timescales [e.g., *Shamberger et al*., 2011]. Further, mean current velocities during the bleaching event were approximately 50% lower compared to the nonbleaching period (Figure 4), and this could have affected the rates of community metabolism. Nevertheless, using multiple-regression analysis with our suite of physical measurements, we found that abiotic factors, including temperature, light, sea level, and current speed, were unable to account for the changes in metabolism (Supporting Information), leaving bleaching as a likely driver. Mean reef-water pH and Ω_{Arag} also declined on average by 0.2 and 0.8 units, respectively, during bleaching (Figure 6). Reef-water chemistry is directly related to the rates of metabolism and to the residence time of water on the reef. Therefore, these changes in carbonate chemistry cannot be ascribed solely to changes in metabolism because the residence time of water on the reef was, on average, twice as long during the bleaching period relative to the nonbleaching period. To illustrate how the changes in metabolism alone would affect reef-water chemistry, we calculated the influence of metabolism on a parcel of water residing on the reef from dawn to dusk under the observed NEC and NEP rates during the bleaching and nonbleaching periods (Figure 9). This analysis shows that bleaching-induced changes in metabolism, primarily the reductions in NEP, were sufficient to reduce maximum daytime $[CO_3^{2-}]$ by ~40%. These effects, which occurred in less than 2 weeks and are comparable to changes predicted for the open ocean by the year 2100 [*Feely et al*., 2009], further highlight that variations in community structure or health strongly modulate reef-water carbonate chemistry.

The tight relationship between NEC and NEP rates was maintained during bleaching and postbleaching (Figure 7), even though the rates were lower during the bleaching event (Figure 5). Several possibilities exist to explain how thermal stress affects NEC and NEP rates together, without decoupling them. If photosynthesis by the symbiotic algae within coral colonies constitutes a significant proportion of the total NEP rate, then the expulsion of these algae from bleached coral colonies could decrease NEP directly. The simultaneous response of NEC may be due to some combination of increasing seawater CO_2 concentrations and direct energetic stress imposed on corals by the loss of their symbionts [*Cohen and Holcomb*, 2009]. Alternatively, symbiont photosynthesis may not contribute substantially to the NEP rates. If this is the case, then the bleaching event potentially reduced NEC directly by perturbing the coral-algal symbiosis, and/or NEP directly by thermal stress on seagrass or fleshy algae [*Campbell et al*., 2006]. Because our metabolic rate data do not identify the relative contributions of various organisms, we cannot determine whether the link between NEC and NEP is established at the organismal level (i.e., the link is driven by the coral-algal symbiosis) or the community level (i.e., the link is driven by interactions between calcifiers and photosynthesizers and is mediated by the seawater carbonate system). Yet whichever is the dominant mechanism, a reduction

in one of the metabolic rates is clearly associated with a reduction in the other (Figures 5 and 7), indicating that they are inextricably linked.

4.3. Implications for Coral Reef Resilience to Ocean Acidification and Warming

A worldwide search is underway to locate the coral reef ecosystems most likely to withstand the effects of climate change into the next century [*Castillo et al*., 2012; *Karnauskas and Cohen*, 2012; *van Hooidonk et al*., 2013; *Shamberger et al*., 2014; *DeCarlo et al*., 2015a]. Our findings imply that anthropogenic CO_2-driven changes in open-ocean chemistry will not necessarily translate directly to changes in reef-water chemistry. Decreases in open-ocean pH and Ω_{Arag} projected by the end of this century ($\sim$0.3 and 1.5, respectively) [*Feely et al*., 2009] are less than the daytime elevation of pH and Ω_{Arag} driven by productivity on Dongsha Atoll. While ocean acidification poses a major threat to coral reef ecosystems, it will not be the sole driver of reef-water carbonate chemistry, nor will it affect all coral reefs equally. Feedbacks between community metabolism and reef-water carbonate chemistry may influence the sensitivity of coral reef ecosystems to acidification of the open ocean, and reefs with high rates of photosynthesis to remove CO_2 from seawater may be the most likely to sustain conditions favorable for rapid calcification. Yet the capacity of benthic communities to modulate reef-water chemistry depends on community structure and health, which are sensitive to thermal stress. By the end of this century, temperatures on more than 80% of the world's reefs are projected to exceed coral bleaching thresholds annually [*van Hooidonk et al*., 2013]. Ocean warming therefore poses an inescapable threat to the metabolic performance of coral reef ecosystems, one that benthic communities cannot buffer.

Acknowledgments

We thank Keryea Soong and the Dongsha Atoll Research Station, the Dongsha Atoll Marine National Park, the crew of the Ocean Researcher 3, Aryan Safie (UC Irvine), and Lisa Hou, Kuo-Yuan Lee, and Yao-Chu Wu (Academia Sinica) for assistance with fieldwork and logistics. The authors are grateful for the constructive and insightful comments of two anonymous reviewers. The data used in this study are presented in Supporting Information. This research was supported by NSF award 1220529 to A.L.C., S.J.L., and K.E.F.S., by the Academia Sinica (Taiwan) through a thematic project grant to G.T.F.W. and A.L.C., and by an NSF Graduate Research Fellowship to T.M.D.

References

Albright, R., C. Langdon, and K. R. N. Anthony (2013), Dynamics of seawater carbonate chemistry, production, and calcification of a coral reef flat, Central Great Barrier Reef, *Biogeosci. Discuss.*, *10*(5), 7641–7676, doi:10.5194/bgd-10-7641-2013.

Albright, R., J. Benthuysen, N. Cantin, K. Caldeira, and K. Anthony (2015), Coral reef metabolism and carbon chemistry dynamics of a coral reef flat, *Geophys. Res. Lett.*, *42*, 3980–3988, doi:10.1002/2015GL063488.

Albright, R., et al. (2016), Reversal of ocean acidification enhances net coral reef calcification, *Nature*, *531*, 362–365, doi:10.1038/nature17155.

Alford, M. H., et al. (2015), The formation and fate of internal waves in the South China Sea, *Nature*, *521*(7550), 65–69, doi:10.1038/nature14399.

Andersson, A. J., and D. Gledhill (2013), Ocean acidification and coral reefs: Effects on breakdown, dissolution, and net ecosystem calcification, *Annu. Rev. Mar. Sci.*, *5*, 321–48, doi:10.1146/annurev-marine-121211-172241.

Andersson, A. J., and F. T. Mackenzie (2011), Ocean acidification: Setting the record straight, *Biogeosci. Discuss.*, *8*, 6161–6190, doi:10.5194/bgd-8-6161-2011.

Andersson, A. J., I. B. Kuffner, F. T. Mackenzie, P. L. Jokiel, K. S. Rodgers, and A. Tan (2009), Net loss of $CaCO_3$ from a subtropical calcifying community due to seawater acidification: Mesocosm-scale experimental evidence, *Biogeosci. Discuss.*, *6*(1), 2163–2182, doi:10.5194/bg-6-1811-2009.

Andersson, A. J., K. L. Yeakel, N. R. Bates, and S. J. de Putron (2014), Partial offsets in ocean acidification from changing coral reef biogeochemistry, *Nat. Clim. Change*, *4*(1), 56–61, doi:10.1038/nclimate2050.

Atkinson, M. J. (2011), Biogeochemistry of nutrients, in *Coral Reefs: An Ecosystem in Transition*, edited by Z. Dubinsky and N. Stambler, Springer, Dordrecht, Netherlands.

Barnes, D. J., and B. Lazar (1993), Metabolic performance of a shallow reef patch near Eilat on the Red Sea, *J. Exp. Mar. Biol. Ecol.*, *174*(1), 1–13, doi:10.1016/0022-0981(93)90248-M.

Bates, N. R., A. Amat, and A. J. Andersson (2010), Feedbacks and responses of coral calcification on the Bermuda reef system to seasonal changes in biological processes and ocean acidification, *Biogeosciences*, *7*(8), 2509–2530, doi:10.5194/bg-7-2509-2010.

Bernstein, W. N., K. A. Hughen, C. Langdon, D. C. McCorkle, and S. J. Lentz (2016), Environmental controls on daytime net community calcification on a Red Sea reef flat, *Coral Reefs*, *35*(2), 697–711, doi:10.1007/s00338-015-1396-6.

Bruno, J. F., H. Sweatman, W. F. Precht, E. R. Selig, and V. G. W. Schutte (2009), Assessing evidence of phase shifts from coral to macroalgal dominance on coral reefs, *Ecology*, *90*(6), 1478–1484, doi:10.1890/08-1781.1.

Campbell, S. J., L. J. McKenzie, and S. P. Kerville (2006), Photosynthetic responses of seven tropical seagrasses to elevated seawater temperature, *J. Exp. Mar. Biol. Ecol.*, *330*(2), 455–468, doi:10.1016/j.jembe.2005.09.017.

Castillo, K. D., J. B. Ries, J. M. Weiss, and F. P. Lima (2012), Decline of forereef corals in response to recent warming linked to history of thermal exposure, *Nat. Clim. Change*, *2*, 756–760, doi:10.1038/nclimate1577.

Cohen, A. L., and M. Holcomb (2009), Why corals care about ocean acidification: Uncovering the mechanism, *Oceanography*, *22*(4), 118–127, doi:10.5670/oceanog.2009.102.

Costanza, R., R. de Groot, P. Sutton, S. van der Ploeg, S. J. Anderson, I. Kubiszewski, S. Farber, and R. K. Turner (2014), Changes in the global value of ecosystem services, *Global Environ. Change*, *26*, 152–158, doi:10.1016/j.gloenvcha.2014.04.002.

Courtney, T. A., et al. (2016), Comparing chemistry and census-based estimates of net ecosystem calcification on a rim reef in Bermuda, *Front. Mar. Sci.*, *3*, 181, doi:10.3389/fmars.2016.00181.

Cyronak, T., I. R. Santos, and B. D. Eyre (2013), Permeable coral reef sediment dissolution driven by elevated pCO_2 and pore water advection, *Geophys. Res. Lett.*, *40*, 4876–4881, doi:10.1002/grl.50948.

Cyronak, T., K. G. Schulz, I. R. Santos, and B. D. Eyre (2014), Enhanced acidification of global coral reefs driven by regional biogeochemical feedbacks, *Geophys. Res. Lett.*, *41*, 5538–5546, doi:10.1002/2014GL060849.

DeCarlo, T. M., K. B. Karnauskas, K. A. Davis, and G. T. F. Wong (2015a), Climate modulates internal wave activity in the Northern South China Sea, *Geophys. Res. Lett.*, *42*, 831–838, doi:10.1002/2014GL062522.

DeCarlo, T. M., A. L. Cohen, H. C. Barkley, Q. Cobban, C. Young, K. E. Shamberger, R. E. Brainard, and Y. Golbuu (2015b), Coral macrobioerosion is accelerated by ocean acidification and nutrients, *Geology*, *43*(1), 7–10, doi:10.1130/G36147.1.
Dickson, A. G., and F. J. Millero (1987), A comparison of the equilibrium constants for the dissociation of carbonic acid in seawater media, *Deep Sea Res., Part A*, *34*(10), 1733–1743, doi:10.1016/0198-0149(87)90021-5.
Doney, S. C., V. J. Fabry, R. A. Feely, and J. A. Kleypas (2009), Ocean acidification: The other CO_2 problem, *Mar. Sci.*, *1*, 169–192, doi:10.1146/annurev.marine.010908.163834.
Dullo, W.-C. (2005), Coral growth and reef growth: A brief review, *Facies*, *51*(1–4), 33–48, doi:10.1007/s10347-005-0060-y.
Falter, J. L., R. J. Lowe, M. J. Atkinson, S. G. Monismith, and D. W. Schar (2008), Continuous measurements of net production over a shallow reef community using a modified Eulerian approach, *J. Geophys. Res.*, *113*, C07035, doi:10.1029/2007JC004663.
Falter, J. L., R. J. Lowe, M. J. Atkinson, and P. Cuet (2012), Seasonal coupling and de-coupling of net calcification rates from coral reef metabolism and carbonate chemistry at Ningaloo Reef, Western Australia, *J. Geophys. Res.*, *117*, C05003, doi:10.1029/2011JC007268.
Feely, R. A., S. C. Doney, and S. R. Cooley (2009), Ocean acidification: Present conditions and future changes in a high-CO_2 world, *Oceanography*, *22*(4), 37–47, doi:10.5670/oceanog.2009.95.
Fu, K. H., Y. H. Wang, L. St Laurent, H. Simmons, and D. P. Wang (2012), Shoaling of large-amplitude nonlinear internal waves at Dongsha Atoll in the northern South China Sea, *Cont. Shelf Res.*, *37*, 1–7.
Garcia, H. E., and L. I. Gordon (1992), Oxygen solubility in seawater: Better fitting equations, *Limnol. Oceanogr.*, *37*(6), 1307–1312, doi:10.4319/lo.1992.37.6.1307.
Gattuso, J.-P., M. Pichon, B. Delesalle, and M. Frankignoulle (1993), Community metabolism and air-sea CO_2 fluxes in a coral reef ecosystem (Moorea, French Polynesia), *Mar. Ecol. Prog. Ser.*, *96*, 259–267.
Gattuso, J.-P., M. Pichon, B. Delesalle, C. Canon, and M. Frankignoulle (1996), Carbon fluxes in coral reefs. I. Lagrangian measurement of community metabolism and resulting air-sea CO_2 disequilibrium, *Mar. Ecol. Prog. Ser.*, *145*, 109–121.
Gattuso, J. P., D. Allemand, and M. Frankignoulle (1999), Photosynthesis and calcification at cellular, organismal and community levels in coral reefs: A review on interactions and control by carbonate chemistry, *Am. Zool.*, *39*(1), 160–183, doi:10.1093/icb/39.1.160.
Gawarkiewicz, G., J. Wang, M. Caruso, S. R. Ramp, K. H. Brink, and F. Bahr (2004), Shelfbreak circulation and thermohaline structure in the northern South China Sea—Contrasting spring conditions in 2000 and 2001, *IEEE J. Ocean. Eng.*, *29*(4), 1131–1143.
Glynn, P. W. (1993), Coral reef bleaching: Ecological perspectives, *Coral Reefs*, *12*(1), 1–17, doi:10.1007/BF00303779.
Golbuu, Y., S. Victor, L. Penland, D. Idip, C. Emaurois, K. Okaji, H. Yukihira, A. Iwase, and R. van Woesik (2007), Palau's coral reefs show differential habitat recovery following the 1998-bleaching event, *Coral Reefs*, *26*(2), 319–332, doi:10.1007/s00338-007-0200-7.
Guo, X., and G. T. F. Wong (2015), Carbonate chemistry in the northern South China Sea shelf-sea in June 2010, *Deep Sea Res., Part II*, *117*, 119–130, doi:10.1016/j.dsr2.2015.02.024.
Ho, D. T., C. S. Law, M. J. Smith, P. Schlosser, M. Harvey, and P. Hill (2006), Measurements of air-sea gas exchange at high wind speeds in the Southern Ocean: Implications for global parameterizations, *Geophys. Res. Lett.*, *33*, L16611, doi:10.1029/2006GL026817.
Hoegh-Guldberg, O., P. J. Mumby, A. J. Hooten, R. S. Steneck, P. Greenfield, E. Gomez, C. D. Harvell, P. F. Sale, A. J. Edwards, and K. Caldeira (2007), Coral reefs under rapid climate change and ocean acidification, *Science*, *318*(5857), 1737–1742, doi:10.1126/science.1152509.
Hönisch, B., A. Ridgwell, D. N. Schmidt, E. Thomas, S. J. Gibbs, A. Sluijs, R. Zeebe, L. Kump, R. C. Martindale, and S. E. Greene (2012), The geological record of ocean acidification, *Science*, *335*(6072), 1058–1063, doi:10.1126/science.1208277.
Johnson, H. K. (1999), Simple expressions for correcting wind speed data for elevation, *Coastal Eng.*, *36*(3), 263–269, doi:10.1016/S0378-3839(99)00016-2.
Jokiel, P. L., C. P. Jury, and K. S. Rodgers (2014), Coral-algae metabolism and diurnal changes in the CO_2-carbonate system of bulk sea water, *PeerJ*, *2*, e378, doi:10.7717/peerj.378.
Karnauskas, K. B., and A. L. Cohen (2012), Equatorial refuge amid tropical warming, *Nat. Clim. Change*, *2*, 530–534, doi:10.1038/nclimate1499.
Kayanne, H., H. Hata, S. Kudo, H. Yamano, A. Watanabe, Y. Ikeda, K. Nozaki, K. Kato, A. Negishi, and H. Saito (2005), Seasonal and bleaching-induced changes in coral reef metabolism and CO_2 flux, *Global Biogeochem. Cycles*, *19*, GB3015, doi:10.1029/2004GB002400.
Key, R. M., A. Kozyr, C. L. Sabine, K. Lee, R. Wanninkhof, J. L. Bullister, R. A. Feely, F. J. Millero, C. Mordy, and T. Peng (2004), A global ocean carbon climatology: Results from Global Data Analysis Project (GLODAP), *Global Biogeochem. Cycles*, *18*, GB4031, doi:10.1029/2004GB002247.
Kinsey, D. W. (1985), Metabolism, calcification, and carbon production: Part I. Systems level studies, paper presented at Fifth International Coral Reef Congress, Int. Assoc. of Biol. Oceanogr., Tahiti, French Polynesia, 27.
Kleypas, J. A., K. R. N. Anthony, and J.-P. Gattuso (2011), Coral reefs modify their seawater carbon chemistry—Case study from a barrier reef (Moorea, French Polynesia), *Global Change Biol.*, *17*(12), 3667–3678, doi:10.1111/j.1365-2486.2011.02530.x.
Kohler, K. E., and S. M. Gill (2006), Coral Point Count with Excel extensions (CPCe): A Visual Basic program for the determination of coral and substrate coverage using random point count methodology, *Comput. Geosci.*, *32*(9), 1259–1269, doi:10.1016/j.cageo.2005.11.009.
Koweek, D., R. B. Dunbar, J. S. Rogers, G. J. Williams, N. Price, D. Mucciarone, and L. Teneva (2015a), Environmental and ecological controls of coral community metabolism on Palmyra Atoll, *Coral Reefs*, *34*(1), 339–351, doi:10.1007/s00338-014-1217-3.
Koweek, D. A., R. B. Dunbar, S. G. Monismith, D. A. Mucciarone, C. B. Woodson, and L. Samuel (2015b), High-resolution physical and biogeochemical variability from a shallow back reef on Ofu, American Samoa: An end-member perspective, *Coral Reefs*, *34*(3), 979–991, doi:10.1007/s00338-015-1308-9.
Kraines, S., Y. Suzuki, and T. Omori (1997), Carbonate dynamics of the coral reef system at Bora Bay, Miyako Island, *Mar. Ecol. Prog. Ser.*, *156*, 1–16, doi:10.3354/meps156001.
Kwiatkowski, L., R. Albright, J. Hosfelt, Y. Nebuchina, A. Ninokawa, T. Rivlin, M. Sesboüé, K. Wolfe, and K. Caldeira (2016), Interannual stability of organic to inorganic carbon production on a coral atoll, *Geophys. Res. Lett.*, *43*(8), 3880–3888, doi:10.1002/2016GL068723.
Langdon, C., and M. J. Atkinson (2005), Effect of elevated pCO_2 on photosynthesis and calcification of corals and interactions with seasonal change in temperature/irradiance and nutrient enrichment, *J. Geophys. Res.*, *110*, C09S07, doi:10.1029/2004JC002576.
Langdon, C., W. S. Broecker, D. E. Hammond, E. Glenn, K. Fitzsimmons, S. G. Nelson, T.-H. Peng, I. Hajdas, and G. Bonani (2003), Effect of elevated CO_2 on the community metabolism of an experimental coral reef, *Global Biogeochem. Cycles*, *17*(1), 1–14, doi:10.1029/2002GB001941.
Langdon, C., J. Gattuso, and A. Andersson (2010), Measurements of calcification and dissolution of benthic organisms and communities, in *Guide to Best Practices for Ocean Acidification Research and Data Reporting*, edited by U. Riebesell et al., Publ. Off. of the Eur. Union, Luxembourg, Europe.
Lantz, C. A., M. J. Atkinson, C. W. Winn, and S. E. Kahng (2014), Dissolved inorganic carbon and total alkalinity of a Hawaiian fringing reef: Chemical techniques for monitoring the effects of ocean acidification on coral reefs, *Coral Reefs*, *33*(1), 105–115, doi:10.1007/s00338-013-1082-5.

Lee, K., L. T. Tong, F. J. Millero, C. L. Sabine, A. G. Dickson, C. Goyet, G. Park, R. Wanninkhof, R. A. Feely, and R. M. Key (2006), Global relationships of total alkalinity with salinity and temperature in surface waters of the world's oceans, *Geophys. Res. Lett.*, *33*, L19605, doi:10.1029/2006GL027207.

Levitus, S. (2010), *NOAA Atlas NESDIS 68-71*, U.S. Gov. Print. Off., Washington, D. C.

Lewis, E., D. Wallace, and L. J. Allison (1998), Program developed for CO_2 system calculations, report, Brookhaven Natl. Lab., Dep. of Appl. Sci., Upton, New York.

Longhini, C. M., M. F. L. Souza, and A. M. Silva (2015), Net ecosystem production, calcification and CO_2 fluxes on a reef flat in Northeastern Brazil, *Estuarine Coastal Shelf Sci.*, *166*, 13–23, doi:10.1016/j.ecss.2014.12.034.

McDougall, T., R. Feistel, and F. Millero (2009), *The International Thermodynamic Equation of Seawater 2010* (TEOS-10): Calculation and Use of Thermodynamic Properties, Global Ship-based Repeat Hydrography Manual, IOCCP Report No, 14, ICPO Publication Series No. 134.

McMahon, A., I. R. Santos, T. Cyronak, and B. D. Eyre (2013), Hysteresis between coral reef calcification and the seawater aragonite saturation state, *Geophys. Res. Lett.*, *40*, 4675–4679, doi:10.1002/grl.50802.

Mehrbach, C., C. H. Culberson, J. E. Hawley, and R. M. Pytkowicx (1973), Measurements of the apparent dissociation constants of carbonic acid in seawater at atmospheric pressure, *Limnol. Oceanogr.*, *18*, 897–907.

Muehllehner, N., C. Langdon, A. Venti, and D. Kadko (2016), Dynamics of carbonate chemistry, production, and calcification of the Florida Reef Tract (2009-2010): Evidence for seasonal dissolution, *Global Biogeochem. Cycles*, *30*, 661–688, doi:10.1002/2015GB005327.

Odum, H., and E. Odum (1955), Trophic structure and productivity of a windward coral reef community on Eniwetok Atoll, *Ecol. Monogr.*, *25*(3), 291–320.

Ohde, S., and R. van Woesik (1999), Carbon dioxide flux and metabolic processes of a coral reef, Okinawa, *Bull. Mar. Sci.*, *65*(2), 559–576.

Roff, G., and P. J. Mumby (2012), Global disparity in the resilience of coral reefs, *Trends Ecol. Evol.*, *27*, 404–413, doi:10.1016/j.tree.2012.04.007.

Sabine, C. L. (2014), Global carbon cycle, in *Encyclopedia of Life Sciences*, John Wiley, Chichester, U. K.

Sarmiento, J., and N. Gruber (2006), *Ocean Biogeochemical Dynamics*, Princeton Univ. Press, Princeton, N. J.

Shamberger, K. E. F., R. A. Feely, C. L. Sabine, M. J. Atkinson, E. H. DeCarlo, F. T. Mackenzie, P. S. Drupp, and D. A. Butterfield (2011), Calcification and organic production on a Hawaiian coral reef, *Mar. Chem.*, *127*(1), 64–75, doi:10.1016/j.marchem.2011.08.003.

Shamberger, K. E. F., A. L. Cohen, Y. Golbuu, D. C. McCorkle, S. J. Lentz, and H. C. Barkley (2014), Diverse coral communities in naturally acidified waters of a western Pacific reef, *Geophys. Res. Lett.*, *41*, 499–504, doi:10.1002/2013GL058489.

Shaw, E. C., B. I. McNeil, and B. Tilbrook (2012), Impacts of ocean acidification in naturally variable coral reef flat ecosystems, *J. Geophys. Res.*, *117*, C03038, doi:10.1029/2011JC007655.

Shaw, E. C., S. R. Phinn, B. Tilbrook, and A. Steven (2014), Comparability of slack water and lagrangian flow respirometry methods for community metabolic measurements, *PLoS One*, *9*(11), e112161, doi:10.1371/journal.pone.0112161.

Shaw, E. C., S. R. Phinn, B. Tilbrook, and A. Steven (2015), Natural in situ relationships suggest coral reef calcium carbonate production will decline with ocean acidification, *Limnol. Oceanogr.*, *60*, 1–12, doi:10.1002/lno.10048.

Shaw, P. T., and S. Y. Chao (1994), Surface circulation in the South China Sea, *Deep Sea Res., Part I*, *41*(11–12), 1663–1683.

Shih, P.-Y., D. Arumugam, and S.-W. Shyue (2011), Bathymetric lidar survey of Penghu Islands and Dongsha Atoll, *Sea Technol.*, *52*(11), 42–45.

Silverman, J., B. Lazar, and J. Erez (2007), Effect of aragonite saturation, temperature, and nutrients on the community calcification rate of a coral reef, *J. Geophys. Res.*, *112*, C05004, doi:10.1029/2006JC003770.

Silverman, J., D. I. Kline, L. Johnson, T. Rivlin, K. Schneider, J. Erez, B. Lazar, and K. Caldeira (2012), Carbon turnover rates in the One Tree Island reef: A 40-year perspective, *J. Geophys. Res.*, *117*, G03023, doi:10.1029/2012JG001974.

Silverman, J., K. Schneider, D. I. Kline, T. Rivlin, A. Rivlin, S. Hamylton, B. Lazar, J. Erez, and K. Caldeira (2014), Community calcification in Lizard Island, Great Barrier Reef: A 33year perspective, *Geochim. Cosmochim. Acta*, *144*, 72–81, doi:10.1016/j.gca.2014.09.011.

Smith, J. E., N. N. Price, C. E. Nelson, and A. F. Haas (2013), Coupled changes in oxygen concentration and pH caused by metabolism of benthic coral reef organisms, *Mar. Biol.*, *160*(9), 2437–2447, doi:10.1007/s00227-013-2239-z.

St Laurent, L. C., H. L. Simmons, T. Y. Tang, and Y. H. Wang (2011), Turbulent properties of internal waves in the South China Sea, *Oceanography*, *24*(4), 78–87.

Takeshita, Y., W. McGillis, E. M. Briggs, A. L. Carter, E. M. Donham, T. R. Martz, N. N. Price, and J. E. Smith (2016), Assessment of net community production and calcification of a coral reef using a boundary layer approach, *J. Geophys. Res. Oceans*, *121*, 5655–5671, doi:10.1002/2016JC011886.

Teneva, L., R. B. Dunbar, D. A. Mucciarone, J. F. Dunckley, and J. R. Koseff (2013), High-resolution carbon budgets on a Palau back-reef modulated by interactions between hydrodynamics and reef metabolism, *Limnol. Oceanogr.*, *58*(5), 1851–1870, doi:10.4319/lo.2013.58.5.1851.

Turk, D., et al. (2015), Community metabolism in shallow coral reef and seagrass ecosystems, lower Florida Keys, *Mar. Ecol. Prog. Ser.*, *538*, 35–52, doi:10.3354/meps11385.

van Hooidonk, R., J. A. Maynard, and S. Planes (2013), Temporary refugia for coral reefs in a warming world, *Nat. Clim. Change*, *3*, 508–511, doi:10.1038/nclimate1829.

Wang, Y. H., C. F. Dai, and Y. Y. Chen (2007), Physical and ecological processes of internal waves on an isolated reef ecosystem in the South China Sea, *Geophys. Res. Lett.*, *34*, L18609, doi:10.1029/2007GL030658.

Wanninkhof, R. (1992), Relationship between wind speed and gas exchange over the ocean, *J. Geophys. Res.*, *97*(C5), 7373–7382, doi:10.1029/92JC00188.

Weiss, R. F. (1974), Carbon dioxide in water and seawater: The solubility of a non-ideal gas, *Mar. Chem.*, *2*(3), 203–215.

Wong, G. T. F., T.-L. Ku, M. Mulholland, C.-M. Tseng, and D.-P. Wang (2007), The south east Asian time-series study (SEATS) and the biogeochemistry of the South China Sea—An overview, *Deep Sea Res., Part II*, *54*(14–15), 1434–1447, doi:10.1016/j.dsr2.2007.05.012.

Yates, K. K., and R. B. Halley (2006), CO_3 concentration and pCO_2 thresholds for calcification and dissolution on the Molokai reef flat, Hawaii, *Biogeosciences*, *3*(3), 357–369, doi:10.5194/bg-3-357-2006.

Yeakel, K. L., A. J. Andersson, N. R. Bates, T. J. Noyes, A. Collins, and R. Garley (2015), Shifts in coral reef biogeochemistry and resulting acidification linked to offshore productivity, *Proc. Natl. Acad. Sci. U. S. A.*, *112*(47), 14,512–14,517, doi:10.1073/pnas.1507021112.

Zeebe, R. E., A. Ridgwell, and J. C. Zachos (2016), Anthropogenic carbon release rate unprecedented during the past 66 million years, *Nat. Geosci.*, *9*(4), 325–329, doi:10.1038/ngeo2681.